Solid State Communications 359 (2023) 115007

Contents lists available at ScienceDirect

Solid State Communications

journal homepage: www.elsevier.com/locate/ssc

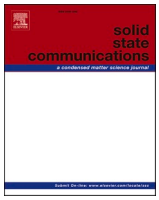

Performance enhancement of CZTS-based solar cells with tungsten disulfide as a new buffer layer

M. Moustafa [a,*], B. Mourched [b], S. Salem [c], S. Yasin [d]

[a] Department of Physics, School of Sciences and Engineering, The American University in Cairo, Cairo, Egypt
[b] College of Engineering and Technology, American University of the Middle East, Kuwait
[c] Department of Basic Engineering Sciences, College of Engineering, Imam Abdulrahman Bin Faisal University, Saudi Arabia
[d] Physics Program, Department of Mathematics, Statistics, and Physics, College of Arts and Sciences, Qatar University, P.O. 2713, Doha, Qatar

ARTICLE INFO

Keywords:
Solar cells
CZTS
Buffer layer
TMDC
WS_2
SCAPS simulation

ABSTRACT

2D layered Transition Metal Dichalcogenide materials (TMDCs) have shown promising potential for ultra-thin photovoltaic and solar cells applications owing to their outstanding photon absorption and electrical and optoelectronics features. This paper intended to discuss a numerical exploration of the CZTS based solar cells employing the solar cell capacitance simulator (SCAPS-1D), using a novel non-toxic *n*-type WS_2 TMDCs as a buffer layer. The cell parameters, such as the thickness and defect density of the CZTS absorber, are optimized. Then, the impact of the energy bandgap (E_g) and the back contact work function of the WS_2 buffer layer on cell performance is investigated. An optimized E_g of 2.2 eV is declared. The results refer to the promoting conduction band alignments at the interface of the buffer absorber (i.e., WS_2/CZTS). Further, we have studied the photovoltaic cell performance versus the defect level of the WS_2 buffer layer. It was resolved that deep defect levels exceeding 1×10^{18} cm^{-3} degrade cell efficiency. The results show an optimized power conversion efficiency of about 26.81% with $V_{oc} = 1.17$ V, $J_{sc} = 27.7$ mA/cm^2, and FF = 83.66%. The simulation was further analyzed and discussed at various operating temperatures. The novel device architecture using WS_2 as a buffer layer might encourage the fabrication of non-toxic CZTS solar cells.

1. Introduction

Solar cells are excellent renewable energy sources needed for the growing energy demand and ensuring green energy. Solar energy or photovoltaics (PV) is universal, environmentally benign, and at no cost, thereby presenting a viable and reliable alternative for exhausted coal and oil resources. Among various PV technologies, thin film-based solar cells show encouraging potential. Across the thin-film-based solar cells, Cu_2ZnSnS_4 (CZTS) has become increasingly popular for photovoltaic devices. They are Kesterite-based, environmentally friendly materials, with all components of the CZTS, such as copper, zinc, and sulfur, being non-toxic and not containing harmful elements like Cd. CZTS is an earth abundant nature of the components of this compound [1]. This solves the problem of the shortage and price issue of Ga, In, and Te elements existing in other corresponding solar cells [1–5]. CZTS solar cells are part of the family of photovoltaic devices with the lowest $/W. Additionally, they have physical properties, including suited direct bandgap energy (E_g) of about 1.50 eV, with p-type conductivity, and an absorption coefficient above 10^4 cm^{-1}, which is reasonable for an absorber material for solar cells [3,6,7]. Indeed, extensive theoretical and experimental work has been reported on the performance of CZTS solar cells, and the enhancement of their efficiency has been widely examined [8–12]. For instance, Shin et al. [13] reported an efficiency of about 8.4%. Sun et al. [14] reported an efficiency of about 9% employing $Zn_{1-x}Cd_xS$ as a buffer layer. Further, over 10% efficiency of the CZTS solar cell was applied by appending a thin layer of Al_2O_3 on the back of the CZTS absorber to boost and refine the band alignment in the Mo contact/CZTS absorber interface [15].

Although CZTS is extensively employed as an absorber material for thin-film solar cells, optimizing the buffer layer and the characteristics of such solar cell structure is still an ongoing research point to enhance its overall performance. In general, the buffer layer represents an essential layer in solar cell structures and plays a key role in optimizing the device performance through band alignment with the absorber layer. It builds a p–n junction, which minimizes the spectrum absorption losses and plays as a bridge to transport the photogenerated charge

* Corresponding author.
E-mail address: mohamed.orabi@aucegypt.edu (M. Moustafa).

https://doi.org/10.1016/j.ssc.2022.115007
Received 24 August 2022; Received in revised form 25 October 2022; Accepted 1 November 2022
Available online 8 November 2022
0038-1098/

carriers from the absorber layer to the electrode. It also reduces the interfacial strain and the defects that might be established by fabricating the window layer. The buffer layer should possess low electrical resistivity, with excellent optical transmittance, accelerating the charge carriers generation process in the absorber layer [16–19]. So far, introducing the most frequently used CdS thin buffer layers is significant in the CZTS thin-film solar cells. However, it contains a toxic Cd. Also, discarding and removing of the cadmium-containing product might cause harm to the environmental conditions. Aside from toxicity, the bandgap value of CdS ranging from 2.40 eV to 2.50 eV might cause a severe photon loss in the short wavelength range, revealing an overall optical absorption drop and consecutively limiting the output performance of solar cells. Thus, much effort has been put into considering alternative materials as buffer layers to replace the conventional CdS [19,20].

Tungsten Disulfide (WS_2) is a Transition Metal that belongs to group IV of the Dichalcogenide materials (TMDC) family. They possess tremendous interest because of their excellent chemical and physical properties and their unique potential benefits for many optoelectronic devices and applications [21–23]. For many reasons, they can be presented as a new buffer layer for the CZTS solar cell. They are identified as quasi-two-dimensional (2D) layered-type materials consisting of a sheet of metal atoms wedged between two chalcogen layers. The adjacent sheets of WS_2 are held together via a weak Van-der-Waals force (VdW) [21–23]. They are semiconductors that exhibit a low lattice mismatch with the absorber materials because of the VdW force. TMDCs are among the most appealing 2D layered materials that can be fabricated with atomic-scale thickness, a remarkable bandgap, and promising electronic and optical properties to replace bulk semiconductors for photovoltaic (PV) applications [23]. The WS_2 has a bandgap of about 1.5 eV–2.2 eV, matching very well within the range of photovoltaic materials, and the conductivity type of WS_2 is reported to be n-type. The high absorption coefficient also distinguishes them. Recently, the ability and capability to develop TMDCs, e.g., ZrS_2 and MoS_2, as a buffer layer for CZTS solar cells, have been discussed [24,25].

This work explores the performance of CZTS-based solar cells using the SCAPS simulation program, using the WS_2 as a novel buffer layer. Initially, the impact of the thickness, the bandgap values, and the defect density of the absorber layer on the device photovoltaic parameters such as open-circuit voltage (V_{oc}), short circuit current density (J_{sc}), fill factor (FF), and the power conversion efficiency (PCE) are discussed. Then, the WS_2 buffer layer optimization is performed regarding bandgap values, defect density, and the back contact work function and their impact on the cell performance. The temperature changes under different atmospheres, so the dependence of solar cell performance on temperature was investigated. Comprehensive knowledge of the CZTS properties by incorporating the new novel buffer layer would promote the design of potential solar cells for taking forward development.

2. Device structure and simulation methodology

In the current study, the simulation was done by the one-dimensional solar cell capacitance simulator (SCAPS) software to study the Mo/CZTS/WS_2/ZnO solar cell device structure [26,27]. Along with the experimental works, it is accepted that numerical modeling and simulations are excellent tools for understanding and optimizing the design of different types of solar cells. SCAPS has shown its capacity to simulate and analyze various photovoltaic cell devices [24,25,28–30]. The solar cell structure and its corresponding band diagram are illustrated in Fig. 1. The structure is built up of the soda-lime glass substrate (SLG), the CZTS as an absorber layer, *n*-type WS_2 as a buffer layer, and ZnO as a window layer. The CZTS and WS_2 form the *p-n* junction of the device. We assume a Hall mobility of about 150 cm^2/Vs at 300 K. The parameters used in simulations are listed in Table 1. They were collected from previous works [25,30–33]. All simulations were carried out at AM 1.5 light spectrum and a light intensity of 1000 W/m^2. After optimizing the CZTS thickness and defect density, the WS_2 buffer layer parameters are investigated deeply. Here, the energy bandgap value of the WS_2 is varied

Table 1
Initial parameters for solar cell structure with WS_2 as a buffer layer.

Parameters	ZnO	WS_2	CZTS	Mo
Thickness (nm)	100	100	500	100
Bandgap (eV)	3.3	2.15	1.50	1.7
Electron affinity (eV)	4.60	4.7	4.50	4.20
Dielectric permittivity	9.0	5.1	13.6	13.6
CB effective density of states (cm^{-3})	2.2×10^{18}	9.7×10^{18}	2.2×10^{19}	2.2×10^{18}
VB effective density of states (cm^{-3})	1.8×10^{19}	1.34×10^{19}	1.8×10^{19}	1.8×10^{19}
Electron thermal velocity (cm/s)	1×10^7	1×10^7	1×10^7	1×10^7
Hole thermal velocity (cm/s)	1×10^7	1×10^7	1×10^7	1×10^7
Electron mobility (cm^2/V.s)	100	100	100	100
Hole mobility (cm^2/V.s)	25	25	25	25
Shallow uniform donor density N_D (cm^{-3})	1×10^{18}	1×10^{18}	0	0
Shallow uniform acceptor density N_A (cm^{-3})	1×10^{14}	1×10^{15}	1×10^{15}	1×10^{14}
Defect density N_t (cm^{-3})	1×10^{14}	1×10^{15}	1×10^{15}	1×10^{15}

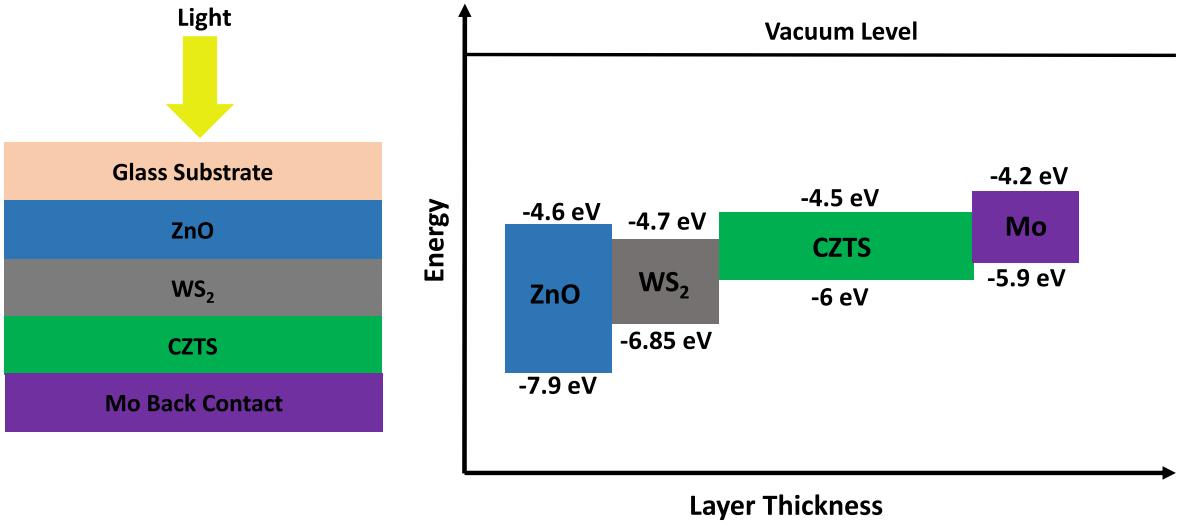

Fig. 1. The modeled solar cell using WS_2 as a new buffer layer and the corresponding energy band diagram.

from 1.5 eV to 2.2 eV. The dependence of the solar cell performance on the back contact work function and the operating temperature is also considered in this study.

3. Results and discussion

Fig. 2 depicts the current-voltage (J–V) characteristics of the Mo/CZTS/WS_2/ZnO solar cell device are using initial layer thicknesses of CZTS, WS_2, and ZnO of 500 nm, 100 nm, and 100 nm, respectively. The rest of the input parameters are listed in Table 1. The initial simulation resulted in the photovoltaic parameters: the V_{oc} of 0.62 V, J_{sc} of 25.48 mA/cm^2, FF of 69.15%, and PCE of 10.98%. The inset of Fig. 2 represents the variation in quantum efficiency (QE) against wavelength. The QE can be used to probe the correlation between the bandgap values and the carrier collection. The QE (λ) is given as the percent of the number of the collected electrons I (λ)/q to the number of incident photons φp (λ), where q is the elementary charge, the I (λ) represents the photogenerated current, and φp (λ) stands for the photon flow. The obtained QE increases in the short wavelength between 400 and 750 nm. A flat spectral response curve is shown for the wavelength between 400 nm and 750 nm. Afterward, it reveals a decrease of QE in the long-wavelength allocated from 750 nm to 830 nm, caused by the incomplete absorption of the long-wavelength photons. The obtained behavior matches prior work well, e.g., Refs. [16,17].

Next step, we move forward with optimizing the proposed CZTS-based solar cell. It has been reported that there is a strong correlation between the solar cells efficiency and the thickness of the absorber layer. In this layer, the absorption of the photons and the generation of the electron-hole pairs take place. Fig. 3(a–d) shows the obtained solar cell performance parameters versus the thickness of the CZTS absorber layer. Here, the thickness has been changed from 100 nm to 1000 nm. Along with the increase of the absorber layer thickness, the J_{sc} enhances, and the efficiency follows almost the same pattern. For instance, the J_{sc} increases from ~13.79 mA/cm^2 to ~26.28 mA/cm^2 as the thickness goes from 100 nm to 600 nm. A rapid increase in the device efficiency is noticed with the increase of the CZTS thickness from 100 nm to 600 nm. Behind this value, no significant improvement is observed. The J_{sc} shows a low increase reaching 27.70 mA/cm^2 at 1000 nm of the absorber thickness. Accordingly, a CZTS thickness greater than 600 nm is indispensable for operating the device at the ultimate efficiency. We achieved optimal performance of an optimal thickness of 1000 nm with a PCE of 11.32%, Jsc of 27.7 mA/cm^2, V_{oc} of 0.61 V, and FF of 67.32%. Increasing the PCE with increasing the absorber layer thickness can be analyzed in the frame of the back contact recombination current density

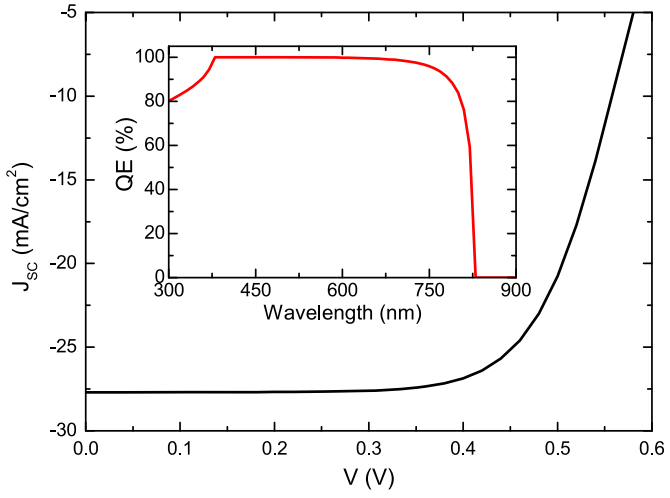

Fig. 2. J-V is the simulated behavior of the Mo/CZTS/WS_2/ZnO solar cell. The inset shows the quantum efficiency (QE) behavior.

and its dependence on the absorber thickness. The thin absorber layer establishes the back contact near the depletion region. A portion of the incoming photons is absorbed nearer to the back contact, notably with lower energy. Thus, partial recombination of the photogenerated carriers will occur at the back contact, resulting in low efficiency. This can be avoided by enhancing the absorber layer thickness. The back contact becomes farther from the depletion region in the thick absorber layer. Thus, the back contact recombination current density gets limited. The depletion width (W_d) of a p-n heterojunction and the theoretically maximum photogenerated current, I_{ph}, can be approximated as in equations (1) and (2), respectively [34,35].

$$I_{ph} = qAG\,(L_e + W_d + L_h) \tag{1}$$

where A, G, L_e, and L_h are the cross-section area of the p-n junction, the generation rate of electron-hole pair, the diffusion length of minority carriers (electrons) in the *p*-side, and the diffusion length of minority carriers (hole) in the *n*-side.

$$W_d = \left[\frac{2\varepsilon_1\,\varepsilon_2\,(V_{bi} - V)\left(N_A^2 + N_D^2\right)}{q\,(\varepsilon_1\,N_D + \varepsilon_2\,N_A)N_D\,N_A}\right]^{1/2} \tag{2}$$

ε_1, ε_2, are the dielectric conductivities. N_D, N_A, V_{bi}, and V are the donor concentration, the acceptor concentration, the built-in voltage, and the applied voltage, respectively. From equation (1), we see that the photogenerated current is proportional to the W_d. The W_d is primarily affected by the absorber thickness. When the W_d is broader, more carrier collection and, consequently more photogenerated current can be achieved, enhancing the output cell performance accordingly. On the other hand, we can not excessively increase the absorber thickness, and optimization is still needed. Because the absorber layer thickness increases further, some incoming photons can be absorbed deep into the absorber layer, further from the depletion region. Consequently, the resulting carriers will not arrive in the space charge region during the allocated lifetime, recombining in the absorber bulk. In Fig. 3 (c) the FF is decreasing with increasing the absorber layer thickness up to 700 nm. Beyond 700 nm, it starts increasing. As the absorber layer thickness increases, series resistance value in the solar cell and the internal power depletion would increase as well, leading to a continuous drop in FF, when the thickness exceeds around 700 nm, FF starts to increase slightly. This increase could be due to a sudden change or instability in the shunt resistance leading to this fine increase beyond 700 nm.

Next, the influence of the defect density on the device performance is studied as depicted in Fig. 4. We have varied the defect density of one layer from 1×10^{13} cm^{-3} to 1×10^{19} cm^{-3} while keeping it constant for the other layers. While the defect density level reflects the layer's quality, it is interesting to recall that defect density is one of the criteria used to control the electronic properties of semiconductors. Chen et al. [36] has reported on the defect properties of CZTS using first-principle calculations. They reported that the formation energy acceptor defects were lower than donor ones. Thus, only a single acceptor-like defects state in the CZTS is introduced. Also, defects density works as trapping centers for the photogenerated charge carriers. Therefore, the process to improve crystallinity and reduce such recombination centers need to be implemented. Referring to Fig. 4, the solar cell performance is strongly influenced by the increase in defects density. The optimal defect density is considered at 1×10^{13} cm^{-3} with a PCE of 14.45%, J_{sc} of 27.7 mA/cm^2, V_{oc} of 0.71 V, and FF of 73.62%. Additionally, the activation energy of the CZTS absorber is less than its bandgap, as shown by Wang et al. [37]. Hence, excessive defects cause detrimental band tailing and potential fluctuations and contribute to the recombination loss mechanism at the buffer/absorber interface, leading to a limit the V_{oc} [38–40]. The results show that high quality (defects density ~10^{15} cm^{-3}) CZTS material is advantageous for CZTS based solar cells devices. Indeed, defects provide recombination pathways, which act as recombination centers that trap the photogenerated carriers. Therefore, their lifetime in the absorbent region is minimized, reducing the photogenerated current

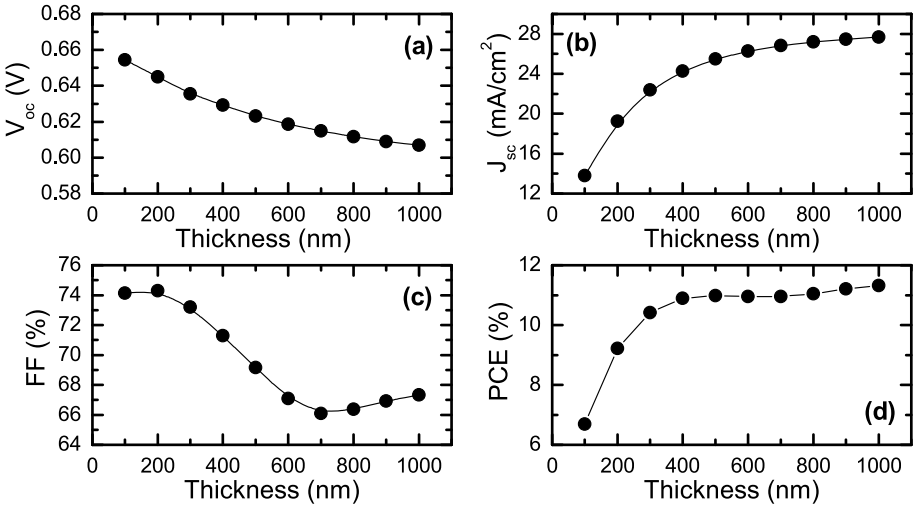

Fig. 3. The solar cell performance parameters versus the CZTS thickness.

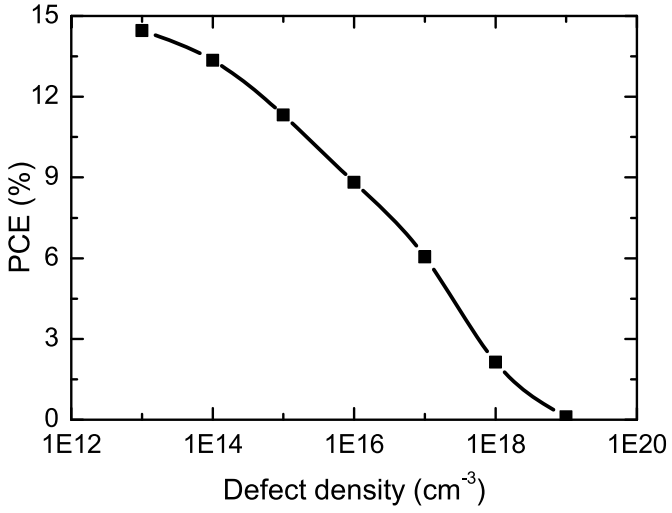

Fig. 4. Impact of CZTS defect density on solar cell efficiency.

density. As the defect level increases, the number of recombination centers increases, as well, and thus the loss in current density becomes more significant, which degrades the conversion efficiency. This is because the light-generated carriers can recombine throughout the energy traps. The process to improve crystallinity and control such recombination centers should be applied and defects below 1×10^{15} cm^{-3} should be governed. This is mainly because the reverse saturation current density increases with increasing the defect level, causing a reduction of V_{oc} and thus the efficiency.

We turn our attention to the newly introduced buffer layer, namely the WS_2 TMDC. Here, the impact of WS_2 on solar cell performance is investigated by the studying effect of its bandgap energy and defects density. The bandgap values of the WS_2 were tuned from 1.1 eV to 2.4 eV. Fig. 5 represents the obtained performance parameters versus the bandgap values of the WS_2. As it is known, the bandgap energy of the buffer layer, among other parameters, directly impacts the conduction band offset (CBO) [41,42]. Among the most suitable approaches to reducing the Voc deficiency in CZTS solar cells is exploring the band alignments at the WS_2-CZTS interface by approaching an optimum CBO. As noticed in Fig. 5, All parameters display an abrupt increase with the increase of the bandgap value of WS_2 from 1.3 eV to 1.8 eV. Increasing the bandgap E_g in this region causes the PCE to increase until it reaches saturation at 1.5 eV, following a stable performance up to $E_g = 1.8$ eV without considerable change in the conversion efficiency can be seen.

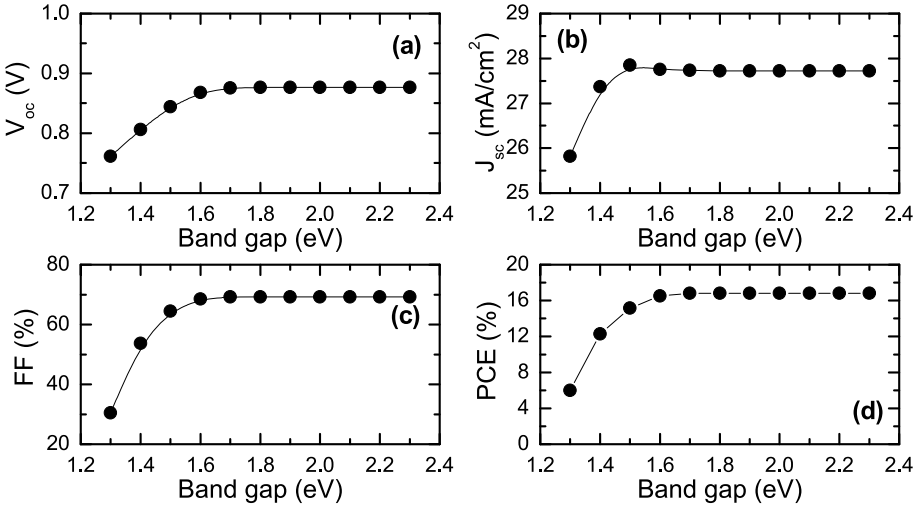

Fig. 5. Impact of variation of the WS_2 bandgap on the solar cell efficiency.

The optimal value for the bandgap of WS_2 is considered at 2.2 eV (corresponding to the reported experimental value) with PCE of 16.83%, J_{sc} of 27.72 mA/cm^2, V_{oc} of 0.88 V, and FF of 69.27%. The V_{oc} increased from 0.76 V at E_g of 1.3 eV to 0.847 V at E_g of 1.5 eV. Beyond a bandgap value of 1.8 eV, the V_{oc} saturates and shows a neglectable decrease. The PCE follows the same pattern improving from 5.99% at 1.3 eV to 15.6% at 1.5 eV. The results might be interpreted by discussing the electronic properties of the interface at the absorber buffer layers in addition to the band offsets. The Conduction Band Offset (CBO) at the absorber/buffer layer plays a vital role in controlling carrier transmission throughout the contact. The amount of this offset is determined by the difference in the absorber/buffer layer's electron affinity. The increase in positive and negative band offsets would respectively form cliff-like and spike-like structures. We assume that the band alignment between the absorber and the buffer is a cliff-like alignment, where the conduction band minimum (CBM) and valence band maximum (VBM) of the WS_2 buffer are lower than their corresponding of the CZTS absorber. This evolves the so-called type-II heterojunction, enhancing the efficient charge separation process as reported experimentally [41,42]. The VBMs of the CZTS and WS_2 are antibonding. With the increase of the bandgap energy, most probably due to an upper shift of the conduction band E_c and a downward shift in the valence band E_v, the value of the conduction band offset (CBO) is decreased. The increase in conduction band offset reflects a decrease in the surface recombination rate. The reduction in the CBO helps to separate the charge, with more accessible promotion electrons are promoted to CB of the *p*-type absorber, and optimum device performance is dominated by the effective transport of electrons across the interface into the *n*-type buffer, and correspondingly enhances the V_{oc}. The concentration of the recombination process (J_R) at the absorber/buffer layer interface can be approximated as [43].

$$J_R = S_h N_v e^{q\varphi_o/k_B T}$$

where S_h represents the hole surface recombination velocity (SRV) in the heterogeneous contact, which is proportional to the density of the interface and capture cross section defects. N_V and φ_o are the valence band density in CZTS and the potential barrier for cavities in the heterogeneous contact, respectively. q stands for the electron charge, and k_BT is the product of the Boltzmann constant and temperature. If this recombination process is considered as the dominant mechanism, V_{oc} is limited to the potential barrier. This might strongly interpret the saturation behavior of the V_{oc} beyond a value of 1.6 eV.

Fig. 6 illustrates the J–V and the quantum efficiency characteristics of the CZTS based solar cell at three selected energy bandgap values of the WS_2 buffer layer. There are no drastic changes in the behavior due to the bandgap change. However, the J-V characteristics support the idea of enhanced behavior for 1.5 eV than for low bandgaps—the V shifts to higher values monotonically. The shift has a clear relationship to the V_{bi}. For this reason, it is recommended to maintain high values of V_{bi}, which leads to a higher output voltage. It is worth noting that from Fig. 6, an improvement in QE was observed.

Fig. 7 shows the effect of the defect density of the WS_2 buffer layer on the solar cell efficiency while keeping the window layer and absorber layer defects constant. We observed that the PCE declines with raising the defects density in the CZTS layer. The efficiency curve shows two different zones. The first zone is where PCE displays stability (of 16.83%) by increasing the defect density of the buffer layer up to 1×10^{18} cm^{-3}. The second one is where PCE decreases with increasing buffer layer defect density, from 10^{18} cm^{-3} to 10^{21} cm^{-3}. The optimal performance is considered at 1×10^{14} cm^{-3} with a PCE of 16.83%. These results show that the WS_2 defect density can maintain enhanced efficiency of CZTS based solar cells for values fewer than 1×10^{18} cm^{-3}. The recombination with the localized energy levels caused by defects can explain the observed degraded performance by increasing the defect density and reducing the conversion efficiency of the solar cell [40].

Interface defects play a dominant role in controlling solar cell output. They play as an energy obstacle limiting the charge carriers from arriving the back contact layer, causing a well-observed reduction in the solar cell efficiency [44]. Fig. 8 shows the impact of the WS_2/CZTS interface defect concentrations on the solar cell performance. Increasing the interface defect density from 10^{13} cm^{-3} to 10^{17} cm^{-3} displayed an aggressive impact on the device's performance. It has been observed

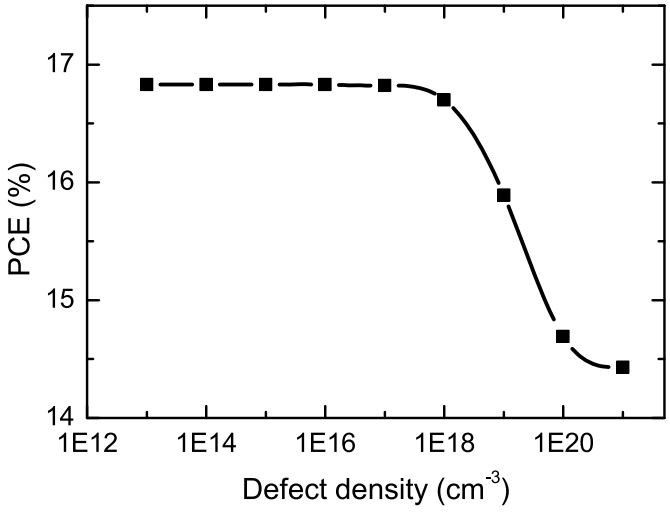

Fig. 7. The impact of the WS_2 defect density on solar cell efficiency.

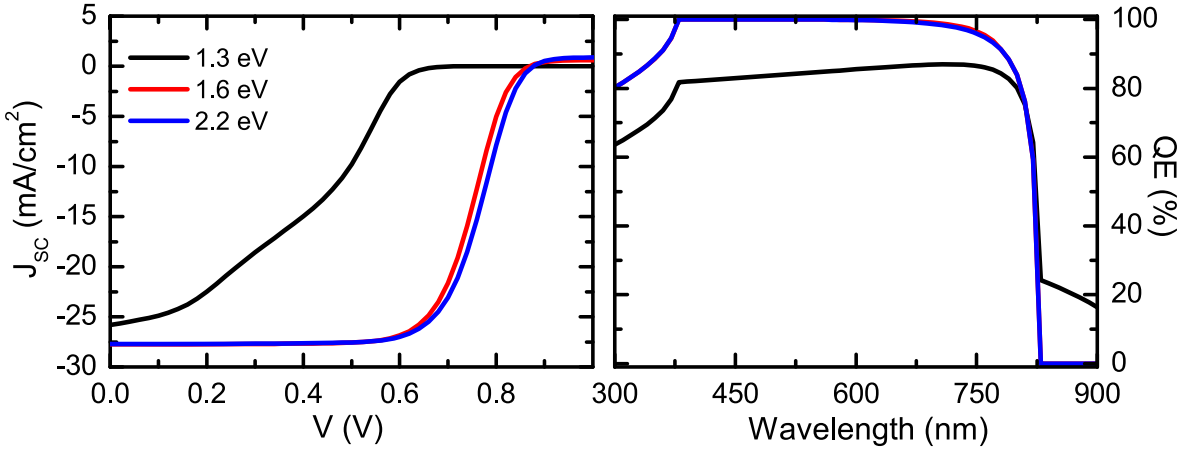

Fig. 6. Left: J-V behavior of the solar cell at different band gap values of WS_2. Right: The corresponding quantum efficiency (QE) behavior at the same conditions.

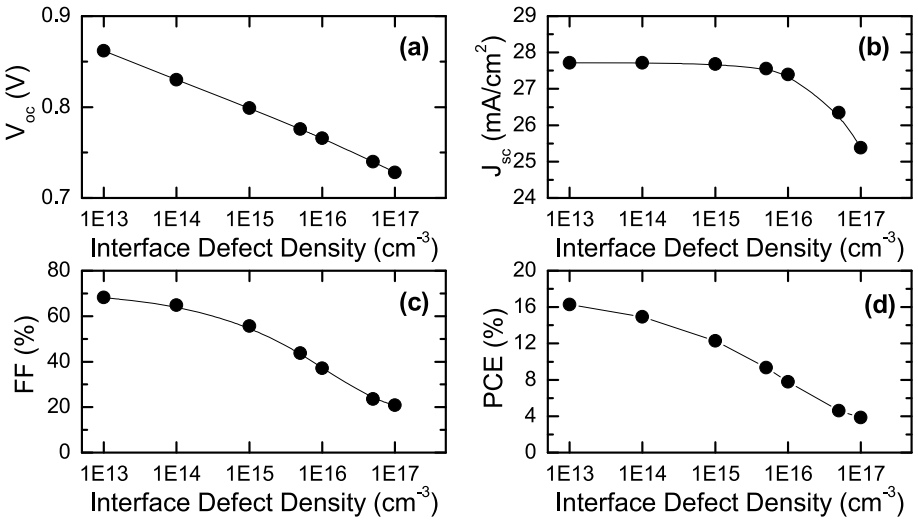

Fig. 8. Effect of the defect density at WS_2/CZTS interface on the solar cell parameters.

that all parameters decrease with increasing defect density. For example, the PCE drops widely from 16.28% to 3.83%. This result is a clear indication that defect density influences the recombination rate of the electron-hole pairs inside the absorber layer, revealing in deterioration in the solar cell performance.

The work function (Φ_m) is a necessary physical quantity that characterizes material surface properties. It plays an essential role in various phenomena such as electron emission from materials and charge transfer at interfaces. Therefore, determining such surface parameters is essential for utilizing the materials understanding, modeling, and fabrication of, for example, Schottky and Ohmic contacts. These parameters strongly influence surface dangling bonds or surface recombination in conventional materials like Si and GaAs. However, in the case of layered TMDC materials, it exhibits chemically saturated surfaces, with less consideration of such complications.

Fig. 9 illustrates the investigated impact of back contact work function Φ_m on solar cell efficiency. The increase in the Φ_m displays a positive impact on solar cell performance [45]. While all parameters increase continuously with increasing Φ_m from 4.7 eV to 5.5 eV, the short circuit current density has a negligible dependence on Φ_m. The efficiency is observed to follow the same trend of the V_{oc}. Above Φ_m = 5.5 eV, the behavior is almost constant. At Φ_m 5.5 eV, a PCE of 26.8%, J_{sc} of 27.71 mA/cm^2, V_{oc} of 1.17 V, and FF of 82.66% are obtained. Several experimental studies have reported results on CZTS based solar cell. However, to our best knowledge, there is no experimental work considering the WS_2 as a buffer layer, however, previous simulation work reports on the performance of tungsten disulfide (WS_2) as an alternative buffer layer for another absorber, i.e., the CdTe solar cell. The optimized structure reported exhibited an efficiency of 20.55% for the interface and bulk defect state density of 10^{10} cm^3 and 10^{13} cm^3, respectively [46]. The obtained results are consistent with our results and can be further discussed as follows. The band alignment at the conduction band of the absorber and buffer is crucial. Electrons from the buffer ($E_{C,buffer}$) layer recombine with the holes of the absorber in the valence band ($E_{V,abs}$), causing interfacial recombination at the CZTS/buffer junction. Reducing the energy difference between absorber ($E_{V,abs}$) and buffer ($E_{C,buffer}$) will increase the recombination. The value of the conduction band offset (ΔE_c) is defined as $\Delta E_c = \chi_2 - \chi_1$, the difference in electron affinity. ΔE_v is the difference in the valence band edges given by $\Delta E_v = (E_{g2}\text{-}E_{g1}) + (\chi_2 - \chi_1)$, where E_g is the bandgap energy. As the Φ_m increases, the valence band offset (ΔE_v) value decreases. The optimization of the Φ_m causes in different energy band offset values for valence and conduction bands directly impacts the potential barrier height at the interface. Therefore, lowering the ΔE_v offset will improve the holes transport and steer to a better energy band alignment, thus improving the electrical contact between them. Thus, a small band offset

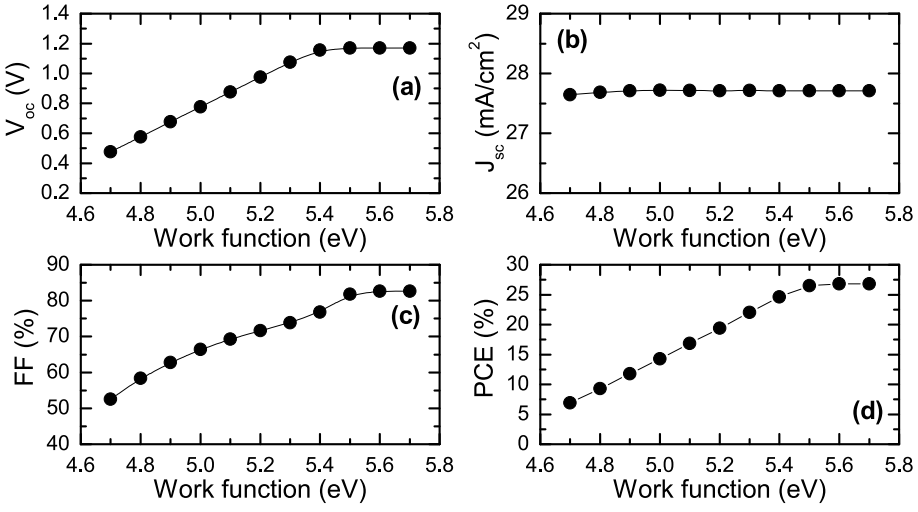

Fig. 9. Impact of back contact work function on the solar cell efficiency.

positive can decrease the recombination and is essential for optimizing the V_{oc} and FF values. It is believed that increasing the work function generally positively impacts solar cell performance by reducing the interface recombination rate. The collection of generated and free carriers can be improved by applying an electric field and providing additional drift to carriers at an appropriate place. The presence of an electric field can be set up using a high–low junction [47]. Since the bandgap of WS_2 is comparable to that of a typical CZTS absorber, it is suggested that it forms a back surface field (BSF) for the photogenerated electrons, offering a low resistivity contact for the holes [45,48]. This BSF is found to help to reduce carrier recombination at the rear contact. It will provide a drift to holes and block electrons at the back contact, which is vital in enhancing cell performance. Increasing the work function is one approach that mediates an ohmic contact to the CZTS and reveals an overall solar cell performance enhancement.

Finally, the effect of the device operating temperature is investigated on the output parameters (PCE and V_{oc}) at a range of temperatures from 250 K to 500 K. The obtained results are illustrated in Fig. 10. As expected, The increasing operating temperature negatively impacts the solar cell device. The V_{oc} the PCE is observed to decrease with the increase in temperature [49]. The coefficient of the voltage variation to temperature $\Delta V_{oc}/\Delta T$ were −0.22%/K. A drop of around 48.6% in the PCE is found with changing the temperature from 240 K to 500 K. An optimal efficiency value of 29.25% is attained at 240 K. With higher temperatures, the electrons gain additional thermal energy. The extensive energy the electrons gain causes them to recombine with holes before getting to the depletion region and collecting. The degradation of PCE with increasing temperature is mainly because of the decrease in the V_{oc}. The observed linear behavior of the PCE with increasing temperature could be interpreted as increasing the dark saturation current with temperature. It has been reported that the darks saturation current in the CZTS based solar cell (~0.2 μA) is higher than other structures (~0.1 nA) for CIGS. With the increase in temperature, the bandgap becomes narrower; and the recombination process of the electrons-holes pair's is accelerated, causing an increase in the darkness current in the cell, hence, lowering the cell performance.

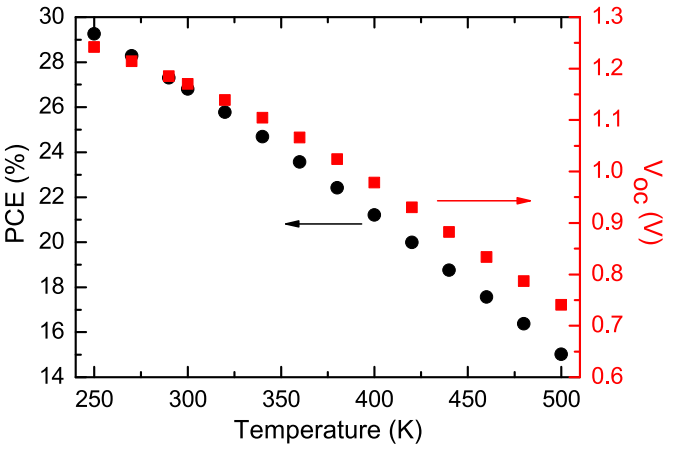

Fig. 10. The operating temperature versus the V_{oc} (right) and the PCE (left) of CZTS based solar cell.

4. Conclusions

In the present work, we study the potentiality of WS_2 as an alternative material to replace the toxic buffer layers (e.g., CdS) to improve the device's performance. We employed a simulation-based approach, using the SCAPS, to enhance the performance of the proposed device structure. The optimization of the absorber layer initiates the study. Next, a comprehensive investigation of the new buffer layer is done. The different photovoltaic parameters were studied versus the thickness, the bandgap energies, and the work function of the structure. Investigating the impact of the defect level of WS_2 declared that a high defect level beyond 1×10^{18} cm^{-3} would shrink the cell performance. The results show an optimized PCE of ~26.81% ($V_{oc} = 1.17$ V, $J_{sc} = 27.7$ mA/cm^2 and FF = 83.66%). These obtained photovoltaic characteristics for the modeled solar cell represents good results with those formerly reported in the literature, particularly when considering a non-toxic WS_2 buffer layer. Furthermore, the operating temperature dependent on the solar cell performance is discussed. The results may be important for optimizing the economical fabrication of Cd-free, non-toxic CZTS kesterite solar cells.

Ethical statement for current applied physics

With this, I Mohamed Moustafa consciously assure that for the Performance Enhancement of CZTS-based Solar Cells with Tungsten disulfide as a new buffer layer, the following is fulfilled:

1. This material is the authors' original work, which has not been previously published elsewhere.
2. The paper is not currently being considered for publication elsewhere.
3. The paper reflects the authors' research and analysis wholly and truthfully.
4. The paper properly credits the meaningful contributions of co-authors and co-researchers.
5. The results are appropriately placed in the context of prior and existing research.
6. All sources used are correctly disclosed (correct citation). Copying of text must be indicated as such by using quotation marks and giving proper references.
7. All authors have been personally and actively involved in substantial work leading to the paper and will take public responsibility for its content Sincerely,

Declaration of competing interest

The authors declare that they have no known competing financial interests or personal relationships that could have appeared to influence the work reported in this paper.

Data availability

No data was used for the research described in the article.

Acknowledgment

The authors thank Marc Burgelman and his colleagues at the University of Gent, Belgium, for granting the free access to SCAPS program.

References

[1] S. Das, Krishna C. Mandal, R. N Bhattacharya, Earth-Abundant $Cu_2ZnSn(S,Se)_4$ (CZTSSe) Solar Cells, vol. 218, Springer Series in Materials Science, 2016, pp. 25–74.
[2] O.K. Simya, A. Mahaboobbatcha, K. Balachander, A Comparative Study on the Performance of Kesterite Based Thin Film Solar Cells Using SCAPS Simulation Program, Superlattices Microstruct, 2015, pp. 248–261.
[3] A.D. Adewoyin, M.A. Olopade, M. Chendo, Prediction and optimization of the performance characteristics of CZTS thin film solar cell using band gap grading, Opt. Quant. Electron. 49 (2017) 336.
[4] J. Crovetto, Andrea, Cu_2ZnSnS_4 Solar Cells: Physics and Technology by Alternative Tracks, DTU Nanotech, 2016.
[5] M.Y. Yeh, P.H. Lei, S.H. Lin, C. D Yang, Copper–Zinc–Tin– Sulfur thin film using spin-coating technology, Materials 9– 7 (2016) 526.
[6] K. Gunavathy, V. Parthibaraj, C. Rangasami, K. Tamilarasan, Prospects of alternate buffer layers for CZTS based thin films solar cells from Numerical Analysis–A Review, South Asian J. Eng. Technol. 2 (2016) 88–96.
[7] D. Cozza, C.M. Ruiz, D. Duche, J.J. Simon, L. Escoubas, Modeling the back contact of $Cu_2ZnSnSe_4$ solar cells, IEEE J. Photovoltaics 6 (2016) 1292–1297.

[8] S. Maklavani, S. Mohammadnejad, The impact of the carrier concentration and recombination current on the p+ pn CZTS thin film solar cells, Opt. Quant. Electron. 52 (2020) 279.

[9] M. Djinkwi Wanda, S. Ouédraogo, J.M.B. Ndjaka, Theoretical analysis of minority carrier lifetime and Cd-free buffer layers on the CZTS based solar cell performances, Optik - Int. J. Light Electron Optics 183 (2019) 284–293.

[10] B. Shin, N.A. Bojarczuk, S. Guha, On the kinetics of $MoSe_2$ interfacial layer formation in chalcogen-based thin film solar cells with a molybdenum back contact, Appl. Phys. Lett. 102 (2013), 091907.

[11] D. Liu, D. Han, M. Huang, X. Zhang, T. Zhang, C. Dai, S. Chen, Theoretical study on the kesterite solar cells based on $Cu_2ZnSn(S, Se)_4$ and related photovoltaic semiconductors, Chin. Phys. B 27 (No. 1) (2018), 018806.

[12] H. Katagiri, K. Jimbo, W.S. Maw, A. Takeuchi, Development of CZTS based thin film solar cells, Thin Solid Films 517 (7) (2009) 2455–2460.

[13] B. Shin, O. Gunawan, Y. Zhu, N.A. Bojarczuk, S.J. Chey, S. Guha, Thin film solar cell with 8.4% power conversion efficiency using an earth-abundant Cu_2ZnSnS_4 absorber, Prog. Photovoltaics 21 (2013) 72.

[14] K. Sun, C. Yan, F. Liu, J. Huang, F. Zhou, J. Stride, M. Green, X. Hao, Over 9% efficient kesterite Cu_2ZnSnS_4 solar cell fabricated by using $Zn_{1-x}Cd_xS$ buffer layer, Adv. Energy Mater. 6 (2016), 1600046.

[15] C. Yan, J. Huang, K. Sun, S. Johnston, Y. Zhang, H. Sun, A. Pu, M. He, F. Liu, K. Eder, L. Yang, J.M. Cairney, N.J. Ekins-Daukes, Z. Hameiri, J.A. Stride, S. Chen, M.A. Green, X. Hao, Cu_2ZnSnS_4 solar cells with over 10 % power conversion efficiency enabled by heterojunction heat treatment, Nat. Energy 3 (2018) 764–772.

[16] F.A. Jhuma, M.Z. Shaily, M.J. Rashid, Towards high-efficiency CZTS solar cell through buffer layer optimization, Mater. Renew. Sustain. Energy 8 (2019) 6.

[17] Md Ali Ashraf, I. Alam, Numerical simulation of CIGS, CISSe and CZTS-based solar cells with In_2S_3 as buffer layer and Au as back contact using SCAPS 1D, Eng. Res. Express 2 (2020), 035015.

[18] C. Platzer-Björkman, J.K. Christoper Frisk, T.E. Larsen, S.-Y. Li, J.J.S. Scragg, J. Keller, F. Larsson, T. Törndahl, Reduced interface recombination in Cu_2ZnSnS_4 solar cells with atomic layer deposition $Zn_{1-x}Sn_xO_y$ buffer layers, Appl. Phys. Lett. 107 (2015), 243904.

[19] Md N. Tousif, S. Mohammad, A.A. Ferdous, Md A. Hoque, Investigation of different materials as buffer layer in CZTS solar cells using SCAPS, J. Clean Energy Technol. 6 (2018) 293.

[20] D. Lee, J. Yup Yang, Investigation of Cu2ZnSnS4 solar cell buffer layer fabricated via spray pyrolysis, Curr. Appl. Phys. 21 (2021) 184–191.

[21] M. Moustafa, A. Paulheim, M. Mohamed, C. Janowitz, R. Manzke, Angle-resolved photoemission studies of the valence bands of ZrS_xSe_{2-x}, Appl. Surf. Sci. 366 (2016) 397–403.

[22] P. Chelvanathan, M. Istiaque Hossain, J. Husna, M. Alghoul, K. Sopian, N. Amin, Effects of transition metal Dichalcogenide molybdenum disulfide layer formation in copper–zinc–tin–sulfur solar cells from numerical analysis, Jpn. J. Appl. Phys. 51 (2012) 10NC32.

[23] S. Roy, P. Bermel, Electronic and optical properties of ultra-thin 2D tungsten disulfide for photovoltaic applications, Sol. Energy Mater. Sol. Cell. 174 (2018) 370–379.

[24] A. Bouarissa, A. Gueddim, N. Bouarissa, H. Maghraoui-Meherezi, Modeling of ZnO/MoS_2/CZTS photovoltaic solar cell through window, buffer and absorber layers optimization, Mater. Sci. Eng. B263 (2021), 114816.

[25] M. Moustafa, T. Al Zoubi, S. Yasin, Exploration of CZTS-based solar using the ZrS2 as a novel buffer layer by SCAPS simulation, Opt. Mater. 124 (2022), 112001.

[26] M. Burgelman, K. Decock, S. Khelifi, A. Abass, Advanced electrical simulation of thin film solar cells, Thin Solid Films 535 (2013) 296–301.

[27] M. Burgelman, P. Nollet, S. Degrave, Modelling polycrystalline semiconductor solar cells, Thin Solid Films (2000) 527–532.

[28] M.O. Moustafa, T. Alzoubi, Numerical simulation of single junction InGaN solar cell by SCAPS, Key Eng. Mater. 821 (2019) 407–413.

[29] S. Yasin, T. Al Zoubi, M. Moustafa, Design and simulation of high efficiency lead-free heterostructure perovskite solar cell using SCAPS-1D, Optik 229 (2021), 166258.

[30] T. AlZoubi, A. Moghrabi, M. Moustafa, S. Yasin, Efficiency boost of CZTS solar cells based on double-absorber architecture: device modeling and analysis, Sol. Energy 225 (2021) 44–45.

[31] A.M. Islam, S. Islam, K. Sobayel, E.I. Emon, F.A. Jhuma, M. Shahiduzzaman, Md Akhtaruzzaman, N. Amin, M.J. Rashid, Performance analysis of tungsten disulfide (WS2) as an alternative buffer layer for CdTe solar cell through numerical modeling, Opt. Mater. 120 (2021), 111296.

[32] S. Enayati Maklavani, S. Mohammadnejad, Enhancing the open-circuit voltage and efficiency of CZTS thin-film solar cells via band-offset engineering, Opt. Quant. Electron. 52 (2020) 72.

[33] K. Sobayel, M. Shahinuzzaman, N. Amin, M.R. Karim, M.A. Dar, R. Gul, M. A. Alghoul, K. Sopian, A.K.M. Hasan, Md Akhtaruzzaman, Efficiency enhancement of CIGS solar cell by WS2 as window layer through numerical modelling tool, Sol. Energy 207 (2020) 479–485.

[34] S.S. Li, p-n junction diodes, in: S.S. Li (Ed.), Semiconductor Physical Electronics, Springer, New York, NY, 2006, pp. 334–380. New York.

[35] M.A. Green, Solar Cells: Operating Principles, Technology, and System Applications, Prentice-Hall, Inc., Englewood Cliffs, NJ, 1982.

[36] S. Chen, J.-H. Yang, X.G. Gong, A. Walsh, S.-H. Wei, Intrinsic point defects and complexes in the quaternary kesterite semiconductor Cu_2ZnSnS_4, Phys. Rev. B 81 (24) (2010), 245204.

[37] K. Wang, B. Shin, K.B. Reuter, T. Todorov, D.B. Mitzi, S. Guha, Structural and elemental characterization of high efficiency Cu_2ZnSnS_4 solar cells, Appl. Phys. Lett. 98 (2011), 051912.

[38] M. Bär, B.-A. Schubert, B. Marsen, R.G. Wilks, S. Pookpanratana, M. Blum, S. Krause, T. Unold, W. Yang, L. Weinhardt, C. Heske, H.-W. Schock, Cliff-like conduction band offset and KCN-induced recombination barrier enhancement at the CdS/Cu_2ZnSnS_4 thin-film solar cell heterojunction, Appl. Phys. Lett. 99 (2011), 222105.

[39] A. Redinger, J. Sendler, R. Djemour, T.P. Weiss, G. Rey, P.J. Dale, S. Siebentritt, Different bandgaps in $Cu_2ZnSnSe_4$: a high temperature coevaporation study, IEEE J. Photovoltaics 5 (2015) 641–648.

[40] S. Campbell, Y. Qu, J. Gibbon, H.J. Edwards, Vin R. Dhanak, D. Tiwari, V. Barrioz, N.S. Beattie, G. Zoppi, Defect limitations in $Cu_2ZnSn(S, Se)_4$ solar cells utilizing an In_2S_3 buffer layer, J. Appl. Phys. 127 (2020), 205305.

[41] M.L.N. Palsgaard, A. Crovetto, T. Gunst, T. Markussen, O. Hansen, K. Stokbro, M. Brandbyge, International Conference on Simulation of Semiconductor Processes and Devices (SISPAD), IEEE, 2016, pp. 377–380, 2016.

[42] Z. Dong, Y. Li, B. Yao, Z. Ding, G. Yang, R. Deng, X. Fang, Z. Weiand L. Liu, An experimental and first-principles study on band alignments at interfaces of Cu_2ZnSnS_4/CdS/ZnO heterojunctions, J. Phys. D 47 (2014), 075304.

[43] G.K. Gupta, A. Dixit, Theoretical studies of single and tandem Cu 2 ZnSn (S/Se) 4 junction solar cells for enhanced efficiency, Opt. Mater. 82 (2018) 11–20.

[44] M.S. Jamala, S.A. Shahahmadi, Mohd Aizat Abdul Wadi, P. Chelvanathan, N. Asim, H. Misran, M.I. Hossain, N. Amin, K. Sopian, Md Akhtaruzzaman, Effect of defect density and energy level mismatch on the performance of perovskite solar cells by numerical simulation, Optik - Int. J. Light Electron Optics 182 (2019) 1204–1210.

[45] A. Kumar and A. D. Thakur, Role of contact work function, back surface field, and conduction band offset in Cu_2ZnSnS_4 solar cell 2018 Jpn. J. Appl. Phys. 57 08RC05.

[46] M. Islam, S. Islam, K. Sobayel, E.I. Emon, F.A. Jhuma, M. Shahiduzzaman, Md Akhtaruzzaman, N. Amin, M.J. Rashid, Performance analysis of tungsten disulfide (WS_2) as an alternative buffer layer for CdTe solar cell through numerical modeling, Opt. Mater. 120 (2021), 111296.

[47] O. von Roos, A simple theory of back surface field (BSF) solar cells, J. Appl. Phys. 49 (1978) 3503.

[48] I.M. Dharmadasa, J.D. Bunning, A.P. Samantilleke, T. Shen, Effects of multi-defects at metal/semiconductor interfaces on electrical properties and their influence on stability and lifetime of thin film solar cells, Sol. Energy Mater. Sol. Cells 86 (2005) 373–384.

[49] M. Abderrezek, M. Fathi, F. Djahli, Comparative study of temperature effect on thin film solar cells, J. Nano- Electron. Phys. 10 (2018).